



This open access document is published as a preprint in the Beilstein Archives with doi: 10.3762/bxiv.2019.99.v1 and is considered to be an early communication for feedback before peer review. Before citing this document, please check if a final, peer-reviewed version has been published in the Beilstein Journal of Organic Chemistry.

This document is not formatted, has not undergone copyediting or typesetting, and may contain errors, unsubstantiated scientific claims or preliminary data.

Preprint Title Synthesis, characterization and structure-property relationships of 1,3-bis(5-substituted-1,3,4-oxadiazol-2-yl)benzenes

Authors Afef Mabrouki, Malek Fouzai, Armand Soldera, Abdelkader Kriaa and ahmed hedhli

Publication Date 03 Sep 2019

Article Type Full Research Paper

Supporting Information File 1 Supplementary Information.docx; 5.1 MB

ORCID® IDs Malek Fouzai - <https://orcid.org/0000-0001-9004-0433>; Armand Soldera - <https://orcid.org/0000-0001-5467-5714>; ahmed hedhli - <https://orcid.org/0000-0001-8541-5958>

Synthesis, characterization and structure-property relationships of 1,3-bis(5-substituted-1,3,4-oxadiazol-2-yl)benzenes

Afef Mabrouki,¹ Malek Fouzai,² Armand Soldera,³ Abdelkader Kriaa,¹ and Ahmed Hedhli*¹

Address: ¹Laboratory of Molecular Organic Chemistry, National Higher Engineering School of Tunis, 5 avenue Taha Hussein, Montfleury, 1089, Tunis, Tunisia, ²LR99ES16 Physics Laboratory of Soft Matter and Electromagnetic Modeling, University of Tunis El Manar, 2092, Tunis, Tunisia, ³Department of Chemistry, Quebec Center for Functional Materials, University of Sherbrooke, Sherbrooke, Québec, Canada J1K 2R1

*Corresponding author

Email: Ahmed Hedhli - ahmed.hedhli@esstt.rnu.tn

Abstract

Two series containing 1,3-bis(1,3,4-oxadiazol-2-yl)benzene as a rigid core (RC) and alkyl or perfluoroalkyl as terminal chains were synthesized and characterized. Liquid Crystal properties of the synthesized compounds have been investigated by Polarizing Optical Microscopy, Differential Scanning Calorimetry and X-ray Diffraction techniques. Conformation effects of the synthesized products on the dipole moments were also investigated.

Keywords

Oxadiazole; dipole moment; liquid crystal; fluorine

Introduction

Liquid-crystalline (LC) materials have been known for over a century [1]. It is clear that architecture and functionalization are essential aspects in molecular engineering of liquid crystals [2]. Introduction of fluorine atom in the molecular structure presents a successful strategy to control the liquid crystal properties. Fluorine element presents the highest electronegativity, the lowest polarizability and a small radius. When bonded to carbon, it forms the strongest single bond in organic chemistry [3]. The C-F bond is highly polarized and this polarity inhibits the lone pair donation from fluorine, making this element a weak coordinator. These properties are the basis for the unique properties of perfluoroalkylated compounds such as high viscosity, high density, high chemical stability, low surface tension, low dielectric constants and low refractive index [4]. The usefulness of these properties makes of fluorine an element of choice for the enhancement of promising properties, remained inaccessible otherwise. However, the combination of small size and high polarity of fluorine atom leads to a subtle modification of properties such as melting point, mesophase morphology, transition temperatures, optical anisotropy, dielectric anisotropy, and visco-elasticity [5-10]. Therefore, many fluorinated liquid crystals have been prepared, and the fluoro-substitution effect has been well studied, especially in the fluoroaromatic derivatives [11–13].

Additionally, the mesomorphic properties of liquid crystals depend strongly on the nature of the terminal chains that are present. Terminal perfluorocarbon chain present in a LC molecule causes stiffening, which generates a lamellar packing and thus contributes to smectic phase

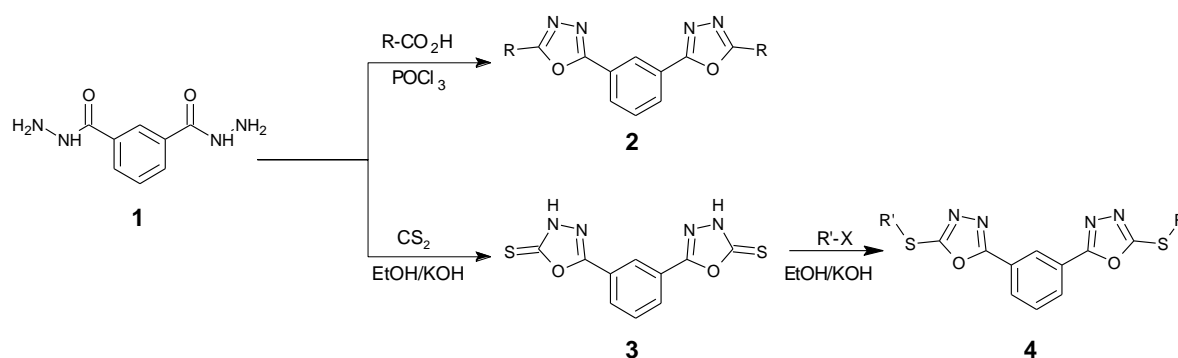
stability [14]. It was reported that even simple *n*-alkanes containing a fluorocarbon block produces smectic phases [15-19]. Some molecules having only a single aromatic ring and fluorinated tail show smectic phases, while their hydrocarbon counterparts are non-mesomorphic [20].

Herein we describe the synthesis and characterization of two series of hydro- and fluorocarbonated 1,3-bis(1,3,4-oxadiazol-2-yl)benzenes. Structure-property relationships of the obtained compounds were investigated.

Results and Discussion

Synthesis

When benzene-1,3-dicarbohydrazide [21] **1** was allowed to react with hydro- or perfluorocarboxylic acids in the presence of phosphorus oxychloride according to standard methods [22], oxadiazole derivatives **2** were obtained (Scheme 1). On the other hand, we converted compound **1** into sulfanyloxadiazole derivatives **4** by treatment with carbon disulfide and subsequent alkylation of the obtained intermediate **3** (Scheme 1).



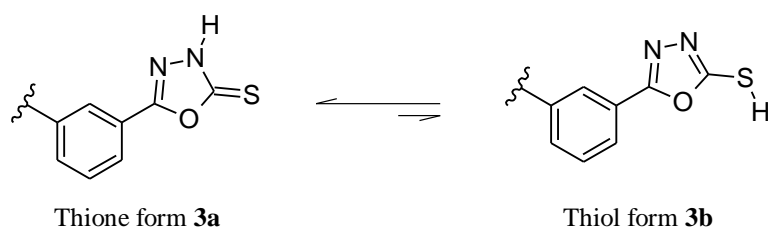
Scheme 1: Synthesis of oxadiazole derivatives **2** and **4**.

Table 1 shows the yields and melting points of the synthesized compounds **2** and **4**.

Table 1: Obtained oxadiazole derivatives **2** and **4**

Cpd.	R / R'	X	Yield (%)	M.p. (°C)	
2	a	C ₆ F ₁₃	-	65	106
	b	C ₇ F ₁₅	-	61	120
	c	<i>n</i> -C ₉ H ₁₉	-	75	83
	d	C ₆ H ₅	-	72	74
4	a	C ₆ F ₁₃ C ₂ H ₄	I	74	128
	b	C ₈ F ₁₇ C ₂ H ₄	I	66	138
	c	<i>n</i> -C ₄ H ₉	Br	70	69
	d	<i>n</i> -C ₁₂ H ₂₅	Br	72	88

The tautomeric equilibrium of compound **3** is illustrated in Scheme 2. On the basis of FT-IR data, it has been concluded that in solution, the equilibrium is shifted to the thione form **3a** rather than the thiol one **3b**. The observed IR absorptions at 3387 cm⁻¹ ($\nu_{\text{N-H}}$) and 1263 cm⁻¹ ($\nu_{\text{C=S}}$) and the absence of absorptions in the 2600-2550 cm⁻¹ region ($\nu_{\text{S-H}}$) support the preference for the thione form in solution. This latter is obviously more solvated than thiol.

**Scheme 2:** Tautomeric equilibrium of compound **3**

Liquid Crystal properties

The structure of compounds **2** and **4** is constituted by a rigid core (three aromatic rings) to which are attached the terminal chains. Based on this structure, some liquid crystalline mesophases were expected. Differential Scanning Calorimetry (DSC), Polarized Optical Microscopy (POM) and X-ray diffraction patterns analysis were used to investigate this behaviour.

DSC measurements

Phase transition temperature (T_t), melting temperatures (T_i) and enthalpy changes (ΔH_t) of compounds **2** and **4** are summarized in Table 2.

Based on data given in Table 2, we found that fluorinated compounds present supplementary transition temperatures compared with the hydrocarbonated analogues.

Table 2: DSC thermograms data of compounds **2** and **4**

Compound	Heating		Cooling		T_i ($^{\circ}\text{C}$)
	T_t ($^{\circ}\text{C}$)	ΔH_t (J/g)	T_t ($^{\circ}\text{C}$)	ΔH_t (J/g)	
2a	115.50	-48.49	85.42	41.61	116.91
2b	115.80	-2.15	103.85	48.13	126.13
	125.11	-50.55			
4a	129.85	-63.76	91.63	1.89	130.81
			98.92	48.33	
4b	118.00	-8.39	96.51	7.21	139.92
	138.41	-41.66	121.13	36.28	
4d	77.10	-133.43	49.24	95.09	78.31

DSC thermograms of fluorinated compounds **2b**, **4a** and **4b** are shown in Figure 1. Thermogram of derivative **2b** presents only one peak between the crystalline and the isotropic phase in cooling. However, it exhibits two peaks in heating which indicates the presence of monotropic intermediate phase between $T=115.8^{\circ}\text{C}$ and $T=125.1^{\circ}\text{C}$ [23]. As it can be seen in the thermogram of compound **4a**, the monotropic liquid crystal mesophase is observed in cooling between $T=91.6^{\circ}\text{C}$ and 98.9°C .

Concerning compound **4b**, the thermogram shows an enantiotropic intermediate phase between 118.0°C and 138.4°C in heating and between 96.5°C and 121.1°C in cooling, indicating a remarkable stabilization in a temperature range of 20°C .

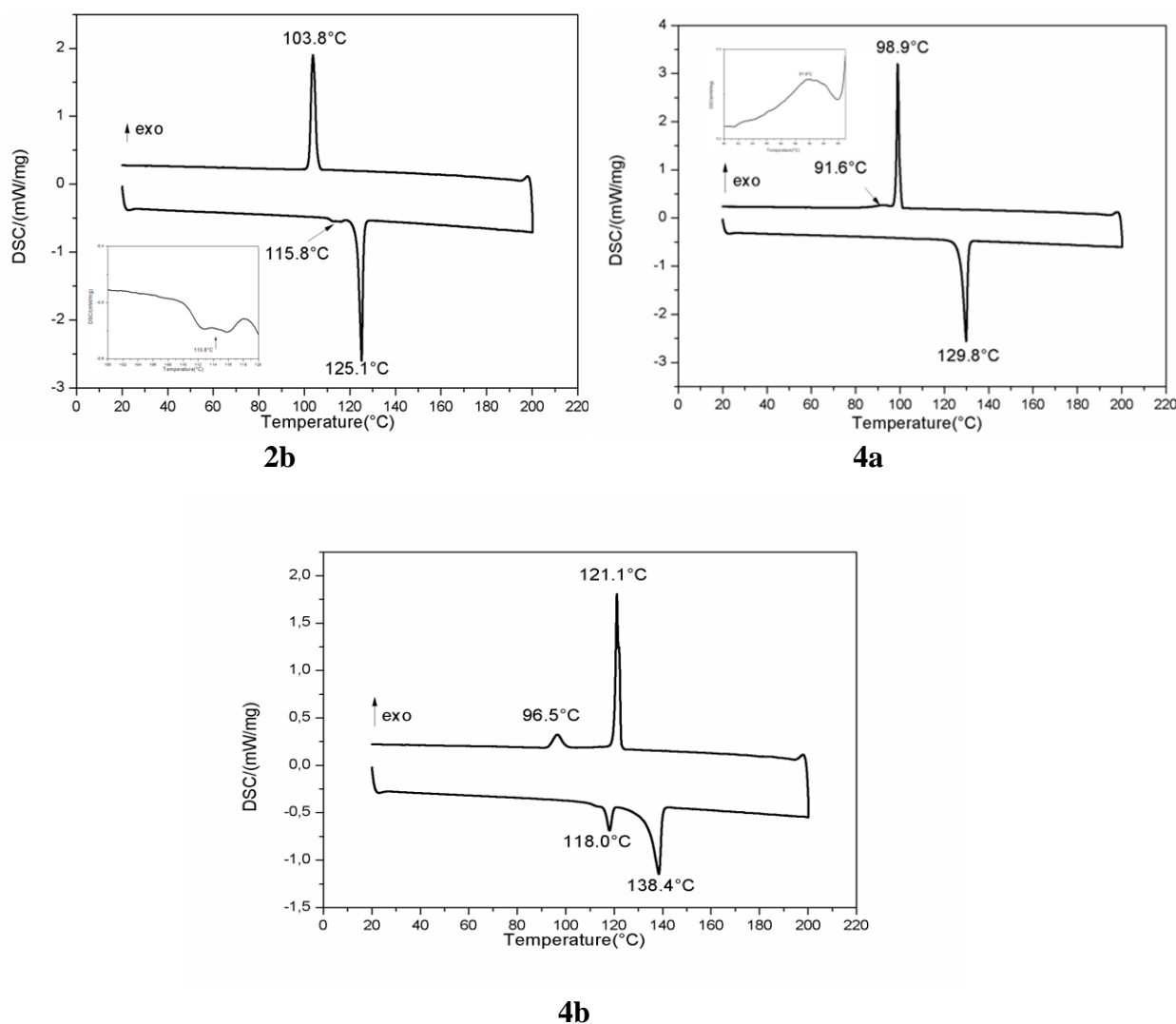


Figure 1: DSC thermograms of fluorinated compounds **2b**, **4a** and **4b** recorded at 5°C/mn at heating (down traces) and cooling (top traces) cycles.

Polarized Optical Microscopy (POM)

In order to achieve a further illustration of the liquid crystal behaviour, POM observations were realized in cooling and heating cycles for compounds **2b**, **4a** and **4b** (Figure 2). POM technique has illustrated smectic phases for all compounds. Identification of the phase textures was accomplished by comparing with those reported in literature.²⁴

The texture of **2b** (Figure 2 (a)) seems to be a variant of focal conic texture with unusually narrow ellipses of a SmA phase. Compound **4a** presents a mosaic SmB phase where the molecules are organized in a hexagonal network as shown in Figure 2(b). The low average of enthalpy value (1.89 J/g) given in Table 2 is due to the first order phase transition marked by the coexistence of the crystalline phase and the liquid crystal phase at least 5°C as it is shown in Figure 2(c). Figure 2(d) shows the POM observation for compound **4b** in heating cycles at

126°C. The texture in cooling is very similar to that in heating; this indicates a remarkable thermodynamic stability of the compound. Based on the texture in Figure 2(d), we can note that the mesophase is hexagonal SmB with strongly double refracting lancets and regions [24].

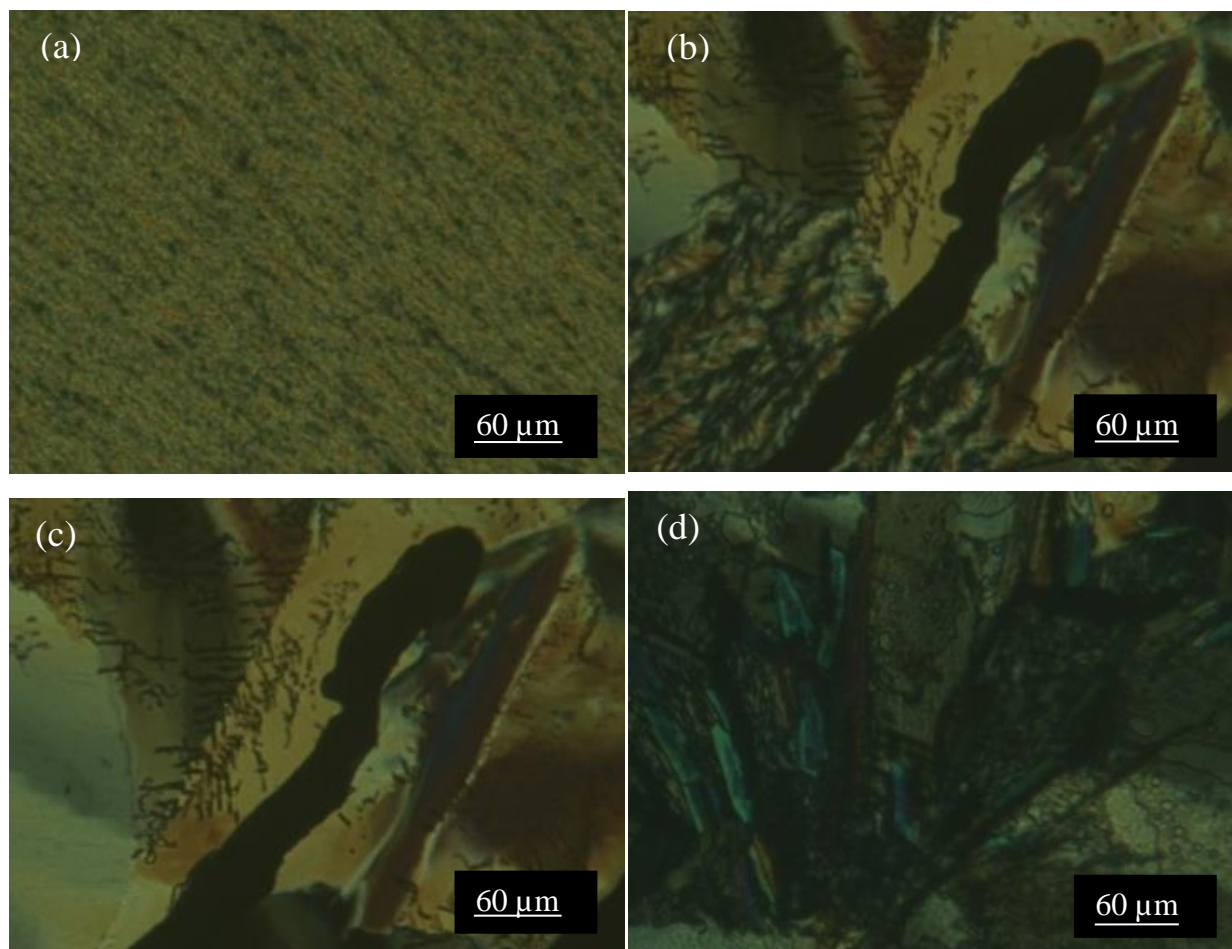


Figure 2: Optical texture (x10) of liquid crystal phase for fluorinated compounds, (a): SmA phase observed in heating at 120°C for compound **2b**; (b): Coexistence between crystalline phase and liquid crystal phase observed in cooling at 91°C for compound **4a**; (c): Mosaic SmB phase observed at 96°C for compound **4a** and (d): SmB phase observed in heating cycle at 126°C for **4b** compound.

X-ray patterns analysis

In order to correlate the obtained results from POM and DSC, we have investigated the X-ray diffraction at the mesophases in cooling and heating cycle of **2b**, **4a** and **4b**. Figure 3 illustrates typical diffraction spectra for compound **2b**. A typical X-ray pattern recorded for

the SmA phase is obtained, it showed two small reflections at 23.69 Å and 15.71 Å at low angle region, and a broad reflection at 5.64 Å. These features are characteristic of SmA phase and are close to data described in the literature [25]. Figure 4 shows a typical X-ray pattern for the hexagonal SmB of **4a** (anyway, we must emphasize that both compounds **4a** and **4b** exhibit identical X-ray pattern). As we can observe, three peaks of diffraction are recorded. The diffraction pattern shows oriented reflections in the small angle region. Bragg peaks at 33.04 Å, and approximately its second- and third order multiples at $d = 16.09$ Å and 10.69 Å, indicate a highly condensed layered structure [26].

However, in the high 2θ -region of Figure 4, slightly different values of the d-spacings calculated from these peaks suggest a weakly distorted hexagonal lattice [26].

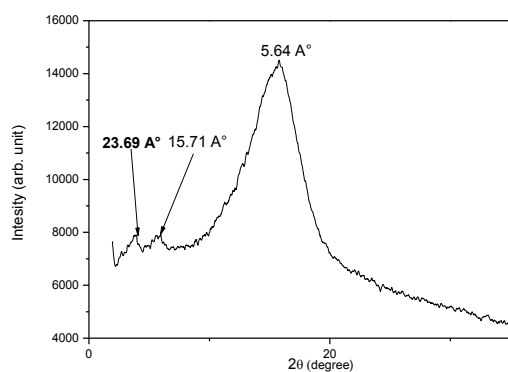


Figure 3: Typical diffractogram observed for compound **2b** at 398K in heating.

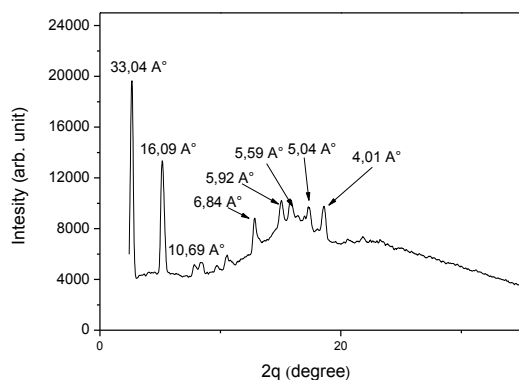


Figure 4: Typical diffractogram observed for compound **4a** at 411K in heating.

Structure-conformation Relationships

Molecular dipole moment

Calculated electric dipole moments of compounds **2** and **4** are reported in Table 3.

Table 3: Calculated dipole moments of **2** and **4**

Compound	Dipole moment (D)			Total
	Components			
	X	Y	Z	
2a	0.08	1.54	-4.48	4.74
2b	-0.04	1.95	-4.30	4.72
2c	-1.20	-3.34	0.71	3.61
2d	-0.93	2.59	0.38	2.78
4a	-1.25	4.35	-0.75	4.58
4b	1.40	5.13	-0.67	5.63
4c	-1.51	0.85	-0.22	1.74
4d	-1.35	0.77	-0.67	1.70

The prepared compounds perform three kinds of conformations, A, B and C. whereas the prepared hydrocarbon derivatives exhibit conformation A (Figure 5(a)), the fluorocarbon analogues adopt, depending on whether they carry linking segment C₂H₄S or not, the conformation B (Figure 5(b)) or C (Figure 5(c)).

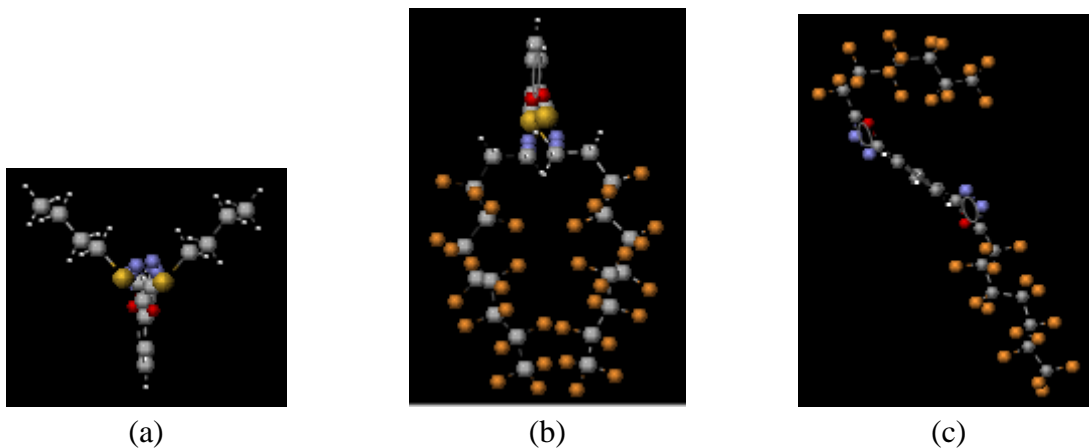


Figure 5: conformer of lowest energy (side-view) of compounds (a): **4c**, conformation A; (b) **4b**, conformation B and (c): **2b**, conformation C. Carbon atoms are shown in gray, hydrogen atoms in white, sulfur atoms in yellow, nitrogen atoms in blue, oxygen atoms in red and fluorine atoms in orange.

In Figure 6 are shown the vector of dipole moment of compounds **4c**, **4b** and **2b**.

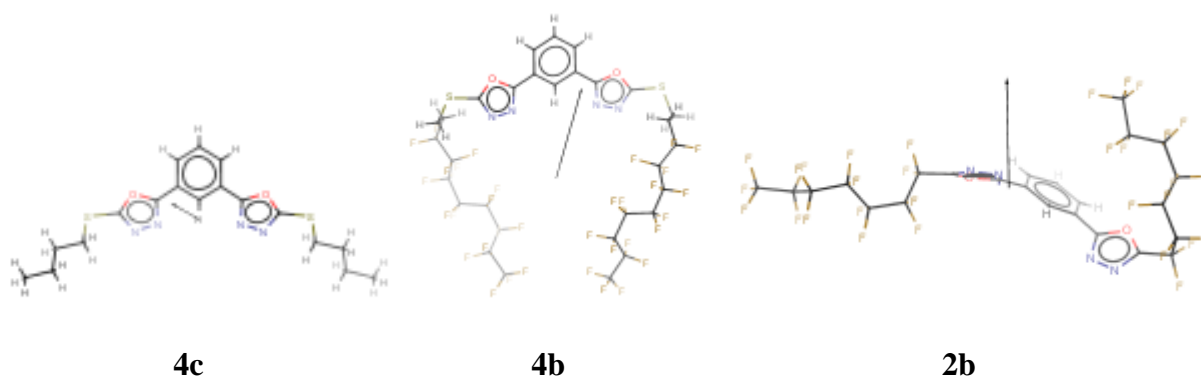


Figure 6: Vector of dipole moment of compounds **4c**, **4b** and **2b**.

In Figure 7 we plotted the calculated dipole moments. To quantify the effect of terminal chains, we calculated dipole moment μ_0 of 1,3-bis(1,3,4-oxadiazol-2-yl)benzene (RC) as it contains no terminal tails and can serve as standard.

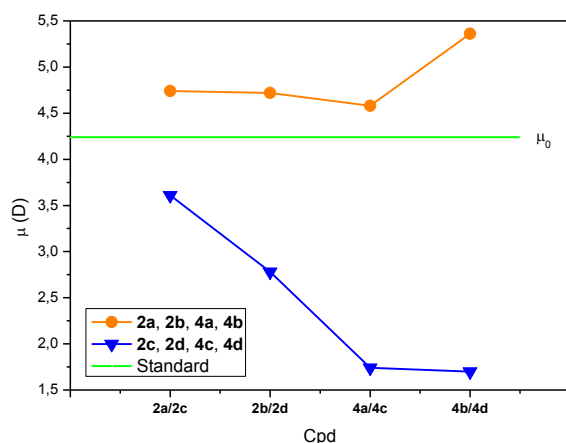


Figure 7: Plot of molecular dipole moments. Orange, fluorocarbon compounds; blue, hydrocarbon compounds; green (horizontal line), dipole moment (μ_0) of RC.

Oxadiazole moieties are thought to be responsible for the majority of the dipole moment in the prepared compounds. Due to the electron-donating effect of alkyl groups in combination with the electron accepting oxadiazole [27], the prepared hydrocarbon compounds are expected to perform dipole moment magnitudes higher than μ_0 . In the fluorinated counterparts, the electron-withdrawing effect of perfluoroalkyl groups would produce the reverse effect leading to a dipole lower than μ_0 . Figure 7 shows an inverse result: the orange plot corresponding to the fluorocarbon derivatives is entirely in the upper side compared to the horizontal green line (standard μ_0), the blue plot of the hydrocarbon derivatives being in the bottom side.

On the other hand, we can note from Figure 5 that the conformation adopted by the hydrocarbon compounds is different from that of the fluorinated homologues, moreover these latter do not adopt the same conformation, according to whether they carry a sulphur atom or not.

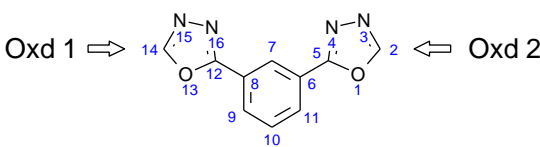
Obviously, the inductive effects alone are inconsistent with the observed results. Hence, we considered the rigid-core (RC) and the terminal chains separately in order to identify a possible interaction between them.

Rigid-core

With three electronegative heteroatoms and only two carbons, the 1,3,4-oxadiazole core has a great electron deficient character. Nevertheless, when incorporated in the rigid-core, the two oxadiazole rings exhibit a slight difference in their electron deficiency.

We depicted in Table 4 the electric charge of heteroatoms in the obtained compounds, as well as those of RC. As shown in Table 4, with the exception of O13, all the other heteroatoms have almost the same electrical charge. The mean value of electric charge for O13 is -0.27. Hence, O13 is highly charged relative to the other heteroatoms, suggesting that Oxd 1 is more polar than Oxd 2.

Table 4: Electric charge of heteroatoms in compounds **2** and **4**

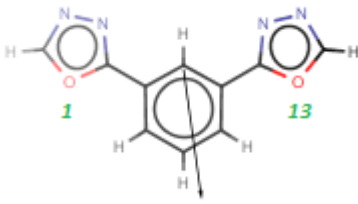


The chemical structure shows a central benzene ring (atoms 7-11) connected to two 1,3,4-oxadiazole rings. The left oxadiazole ring has atoms 12, 13, 14, 15, and 16. The right oxadiazole ring has atoms 1, 2, 3, 4, and 5. Dipole moment arrows are shown pointing from the left oxadiazole ring towards the right oxadiazole ring, labeled 'Oxd 1' and 'Oxd 2'.

Cpd.	O13	N15	N16	O1	N4	N3
2a	-0.25	-0.14	-0.10	-0.16	-0.14	-0.13
2b	-0.25	-0.14	-0.10	-0.16	-0.14	-0.13
4a	-0.28	-0.14	-0.13	-0.15	-0.13	-0.12
4b	-0.28	-0.14	-0.13	-0.15	-0.13	-0.12
2c	-0.29	-0.17	-0.12	-0.18	-0.15	-0.15
2d	-0.26	-0.16	-0.13	-0.18	-0.15	-0.15
4c	-0.28	-0.14	-0.13	-0.15	-0.13	-0.12
4d	-0.28	-0.14	-0.13	-0.15	-0.13	-0.12
Mean value	-0.27	-0.15	-0.12	-0.16	-0.14	-0.13
RC	-0.28	-0.16	-0.11	-0.18	-0.15	-0.15

Such a difference in polarity was corroborated by the direction of the dipole moment of RC (Table 5). Therefore, it is not surprising to find the molecular electron-deficient center so far from the axis of the molecule in the prepared compounds.

Table 5: Dipole moment of RC

Compound	μ (D)			
	X	Y	Z	Total
 RC	0.59	-4.20	-0.01	4.24

Terminal chains

The intrinsic difference between fluorocarbon and hydrocarbon chains has to be taken into account to elucidate the conformational arrangements of the prepared compounds.

Because of electrostatic repulsions of fluorine atoms in the relative 1,3-positions in the crystalline state, perfluorocarbon chain adopt a helical conformation of the carbon backbone [28]. The cylinder-like structure of the segment $(CF_2)_m$ resembles a stiff rod in which the carbon skeleton is covered by fluorine atoms. In the hydrocarbon counterpart the segment $(CH_2)_n$ adopts the typical in-plane zigzag conformation [28].

Fluorine is the most electronegative element of the periodic table. This high electronegativity confers to C—F bond a large dipole moment of 1.39 D while that of C—H bond is only 0.40 D [29]. Owing to the all-*trans* conformation, the local dipole moments $C^{\delta-}-H^{\delta+}$ of hydrocarbon chain are mutually neutralized. In $(CF_2)_m$ segment, Hasegawa *et al* noted that the local dipoles $C^{\delta+}-F^{\delta-}$ cannot be cancelled out and the surface of fluorocarbon chain remains polar [30].

Interaction rigid core-terminal chains

The typical model for aromatic electron Donor-Acceptor (D-A) interactions was established by Hunter and Sanders in 1990 [31]. According to this model, benzene and hexafluorobenzene form a complex where benzene is the donor (electron-rich) and hexafluorobenzene is the acceptor (electron-deficient). Experimental evidence for this complex was first reported in 1960 [32]. The electron D-A concept may be regarded as Lewis base-Lewis acid type or charge-transfer.

Based upon the above considerations, we could attribute the close proximity of fluorinated chains in conformation B to a through space electron D-A intramolecular interaction between the perfluoroalkyl chains (electron-rich moieties) and the electron-deficient center of the molecule. The two fluorocarbon chains are symmetrically arranged with respect to the origin of the vector of dipole moment (Figure 6, compound **4b**). In compound **4b**, which adopts the conformation B (Figure 5(b)), the fluorinated terminal chains resemble a twin [33]. The molecule is linear in the meaning that the rigid-core is in one side and the two arms in the other. Thus arranged, the molecule is polar and performs liquid crystal phases.

The presence of the linking group C_2H_4S in compounds **4a** and **4b** has the desired effect of increasing conformational flexibility, bringing the two fluoroalkyl chains closer. As a result, **4a** and **4b** adopt the conformation B (Figure 5(b)). However, although the non-fluorinated analogues **4c** and **4d** also carry the segment C_2H_4S , the electron D-A interaction was not observed in these compounds, obviously because of the fundamental difference between fluoro- and hydrocarbon chains mentioned above. The conformation A adopted by these compounds (Figure 5(a)) lowers the dipole moments and thereby precludes mesophases formation.

On the other hand, direct linkage of perfluoroalkyl group to the rigid-core makes the system more rigid. As shown in Figure 5(c), the conformation C adopted by compound **2b** is quite different from conformation B described above. While R_F2 (R_F linked to Oxd 2) folds to interact with the molecular electron-deficient center according to an electron D-A interaction, R_F1 (R_F linked to Oxd 1) remains straight. The dipole moment of compound **2b** (Figure 6) originates close Oxd 1. With the presumption that the molecular electron-deficient center is near the origin of the vector, we can attribute the absence of folding on the Oxd 1 side to the huge strain that R_F1 must undergo to interact with a center that is so close to it.

Conclusion

In this paper we have described the preparation and characterization of two new series of 2,2'-(1,3-phenylene) bis(1,3,4-oxadiazole) derivatives bearing different hydro- and fluorocarbonated chains. Structures of the obtained compounds were established by usual spectroscopic techniques. DSC, POM and X-ray diffraction investigations evidence the

existence of the liquid crystal mesophase in the perfluorinated derivatives whereas the hydrocarbonated counterparts just present a thermotropic character. The dipole moment-molecular conformation relationship was scrutinized in order to elucidate the role of the molecular conformation on the dipole moment magnitude. Since some of the studied compounds show mesomorphic properties, it is important to lead on a deep study in order to investigate other parameters such as response time, viscosity and dielectric anisotropy.

Supporting Information

Supporting Information

Experimental details, compound characterization data, copies of ^1H , ^{13}C NMR and IR spectra.

Acknowledgements

We acknowledge ChemAxon Ltd (<https://chemaxon.com>) for the academic license agreement. We thank Mr Nicolas Couvrat from the Rouen University for helping DSC measurements. The authors are thankful to The Ministry of Higher Education and Scientific Research for funding and support.

References

1. Demus, D. J.; Goodby, J.; Gray, G. W.; Spiess, H. W.; Vill, V. *Handbook of Liquid Crystals set* (Wiley-VCH), **1998**.
2. Zuev, V. V. *Mol. Cryst. Liq. Cryst.* **2011**, 537, 103-107
[doi:10.1080/15421406.2011.556513](https://doi.org/10.1080/15421406.2011.556513)
3. Chambers, R. D. *Fluorine in organic Chemistry* (Wiley: New York), **1973**.
4. Hird, M. *Chem. Soc. Rev.* **2007**, 36, 2070-2095. [doi:10.1039/B610738A](https://doi.org/10.1039/B610738A)
5. Hird, M.; Toyne, K. J. *Mol. Cryst. Liq. Cryst.* **1998**, 323, 1-67.
[doi:10.1080/10587259808048432](https://doi.org/10.1080/10587259808048432)
6. Kirsch, P.J. *Fluorine. Chem.* **2015**, 177, 29-36. [doi:10.1016/j.jfluchem.2015.01.007](https://doi.org/10.1016/j.jfluchem.2015.01.007)
7. Guittard, F.; Geribaldi, S. *J. Fluor. Chem.* **2011**, 107, 363-374.
[doi: 10.1016/S0022-1139\(00\)00380-8](https://doi.org/10.1016/S0022-1139(00)00380-8)

8. Kirsch, P.; Lenges, M.; Ruhl, A.; Huber, F.; Chambers, R. D.; Sandford, G. *J. Fluor. Chem.* **2007**, *128*, 1221-1226. [doi:10.1016/j.jfluchem.2007.04.010](https://doi.org/10.1016/j.jfluchem.2007.04.010)
9. Guittard, F.; Taffin, G. E.; Garibaldi, S.; Cambon, A. *J. Fluorine Chem.* **1999**, *100*, 85-96. [doi:10.1016/S0022-1139\(99\)00205-5](https://doi.org/10.1016/S0022-1139(99)00205-5)
10. Tschierske, C. *Top. Curr. Chem.* **2012**, *318*, 1-108. [doi:10.1007/128_2011_267](https://doi.org/10.1007/128_2011_267)
11. Yoshinori, I.; Masakazu, K.; Tetsuo, K.; Sadao, T.; Kiyofumi, T.; Haruyoshi, T. *SID Int. Symp. Dig. Tech. Pap.* **2001**, *8*, 959-961. [doi:10.1889/1.1832031](https://doi.org/10.1889/1.1832031)
12. Kirsch, P.; Huber, F.; Lenges, M.; Taugerbeck, A. *J. Fluor. Chem.* **2011**, *112*, 69-72. [doi:10.1016/S0022-1139\(01\)00488-2](https://doi.org/10.1016/S0022-1139(01)00488-2)
13. Catalano, D.; Geppi, M.; Marini, A.; Veracini, C. A.; Urban, S. J.; Czub, J.; Kuczynski W.; Dabrowski, R. *J. Phys. Chem. C.* **2007**, *111*, 5286-5299. [doi:10.1021/jp066710u](https://doi.org/10.1021/jp066710u)
14. Ivashchenko, A. V.; Kovshev, E. I.; Lazareva, V. T.; Prudnikova, E. K.; Titov, V. V.; Zverkova, T. I.; Barnik, M. I.; Yagupolski, L. M. *Mol. Cryst. Liq. Cryst.* **1981**, *67*, 235-240. [doi:10.1080/00268948108070893](https://doi.org/10.1080/00268948108070893)
15. Viney, C.; Russell, T. P.; Depero, L. E.; Twieg, R. *Mol. Cryst. Liq. Cryst.* **1989**, *168*, 63-82. [doi:10.1080/00268948908045960](https://doi.org/10.1080/00268948908045960)
16. Viney, C.; Twieg, R. J.; Russell, T. P.; Depero, L. E. *Liq. Cryst.* **1989**, *51*, 1783-1788. [doi:10.1080/02678298908045688](https://doi.org/10.1080/02678298908045688)
17. Viney, C.; Twieg, R. J.; Gordon, B. R.; Rabolt, J. F. *Mol. Cryst. Liq. Cryst.* **1991**, *198*, 285-289. [doi:10.1080/00268949108033404](https://doi.org/10.1080/00268949108033404)
18. Twieg, R. J.; Rabolt, J. F. *Macromolecules* **1988**, *21*, 1806-1811. [doi:10.1021/ma00184a045](https://doi.org/10.1021/ma00184a045)
19. Rabolt, J. F.; Russell, T. P.; Twieg, R. J. *Macromolecules* **1984**, *17*, 2786-2794. [doi:10.1021/ma00142a060](https://doi.org/10.1021/ma00142a060)
20. Johansson, G.; Percec, V.; Ungar, G.; Smith, K. *Chem. Mater.* **1997**, *9*, 164-175. [doi:10.1021/cm960267q](https://doi.org/10.1021/cm960267q)
21. Eissa, H. H. *Org. Chem. Curr. Res.* **2013**, *2*, 1-8. [doi: 10.4172/2161-0401.1000122](https://doi.org/10.4172/2161-0401.1000122)
22. De Oliveira, C. S.; Lira, B. F.; Barbosa-Filho, J. M.; Lorenzo, J. G. F. De Athayde-Filho, P. F. *MOLECULES* **2012**, *17*, 10192-10231. [doi:10.3390/molecules170910192](https://doi.org/10.3390/molecules170910192)
23. Pardey, R.; Zhang, A.; Gabori, P. A.; Harris, F. W.; Cheng, S. Z.; Adduci, J.; Facinelli, J. V. Lenz, R. W. *MACROMOLECULES* **1992**, *25*, 5060-5068. [doi:10.1021/ma00045a036](https://doi.org/10.1021/ma00045a036)
24. Demus, D.; Richter, L. *textures of liquid crystals* (VEB Deutscher Verlag für Grundstoffindustrie, Leipzig) **1980**.

25. Yuvaraj, A. R.; Mashitah, M. Y.; Lutfor R. *Mol. Cryst. Liq. Cryst.* **2016**, *631*, 21-30. [doi:10.1080/15421406.2016.1147328](https://doi.org/10.1080/15421406.2016.1147328)
26. Repasky, P. J.; Kooijman, D. M. A.; Kumar, S.; Hartley, C. S. *J. Phys. Chem. B.* **2016**, *120*, 2829-2837. [doi:10.1021/acs.jpcc.5b10990](https://doi.org/10.1021/acs.jpcc.5b10990)
27. Malek, K.; Zborowski, K.; Gebski, K.; Proniewicz, L. M.; Schroeder, G. *Mol. Phys.* **2008**, *106*, 1823-1833. [doi:10.1080/00268970802317512](https://doi.org/10.1080/00268970802317512)
28. Bunn, C. W. Howells, E. R. *NATURE*, **1954**, *174*, 549. [doi:10.1038/174549a0](https://doi.org/10.1038/174549a0)
29. Minkin, V. I.; Osipov, O. A.; Zhdanov, Y. A. *Dipole Moments in Organic Chemistry* (Plenum Press, New York), **1970**.
30. Hasegawa, T.; Shimoaka, T.; Shioya, N.; Morita, K.; Sonoyama, M.; Takagi, T.; Kanamori, T. *ChemPlusChem.* **2014**, *79*, 1421-1425. [doi:10.1002/cplu.201402156](https://doi.org/10.1002/cplu.201402156)
31. Hunter, C. A.; Sanders, J. K. M. *J. Am. Chem. Soc.* **1990**, *112*, 5525-5534. [doi:10.1021/ja00170a016](https://doi.org/10.1021/ja00170a016)
32. Patrick, C. R.; Prosser, G. S. *NATURE* **1960**, *187*, 1021. [doi:10.1038/1871021a0](https://doi.org/10.1038/1871021a0)
33. Hird, M. *Liq. Cryst. Today* **2005**, *14*, 9-21. [doi:10.1080/14645180500274347](https://doi.org/10.1080/14645180500274347)